3 Ionization and the Saha Equation

Ionization balance also critically affects the strengths of atomic de-excitation lines, constraining the number of states available for de-excitation. Such ionization balance also depends strongly on Boltzmann factors.

C & O, pp. 213–6

Let χ_i be the ionization energy for transitioning from ionization state i to state $i+1$. Thus, for $HI \to HII$, $\chi_I = 13.6\,\mathrm{eV}$.

• We define the **partition function** Z_i to be the weighted sum of the number of ways an atom or ion ionization state i can arrange its electrons among excitation states. Boltzmann statistics then gives

$$Z_i \;=\; g_1 + \sum_{j=2}^{\infty} g_j \; e^{-(E_{i,j}-E_{i,1})/kT} \tag{7}$$

for the g_i being the degeneracy factors ($g_1 = 2$, $g_2 = 8$, etc.; $g_n = 2n^2$).

• The ratio of the number N_{i+1} of atoms in ionization state $i+1$ to the number N_i in state i is given by detailed balance and is

$$\boxed{\frac{N_{i+1}}{N_i} \;=\; \frac{2Z_{i+1}}{n_e Z_i}\left(\frac{m_e kT}{2\pi\hbar^2}\right)^{3/2} e^{-\chi_i/kT} \quad .} \tag{8}$$

This is the **Saha Equation**, derived in 1920. The factor of 2 accommodates the two spin states of free electrons, and represents their partition function (i.e. no bound states).

• e.g. For pure hydrogen gas, $Z_{II} = 1$ since protons have no degeneracy, *in the atomic sense*, and $Z_I \approx g_1 = 2$ for $kT \ll E_2 - E_1$. Then

$$\frac{N_{II}}{N_I} \;=\; \frac{1}{n_e}\left(\frac{m_e kT}{2\pi\hbar^2}\right)^{3/2} e^{-13.6\mathrm{eV}/kT} \quad . \tag{9}$$

This applies to temperatures $T \lesssim 3\times 10^4\,\mathrm{K}$ and evinces an abrupt transition from neutrality to virtually complete ionization at $10^4\,\mathrm{K}$.

Boltzmann and Saha Equations

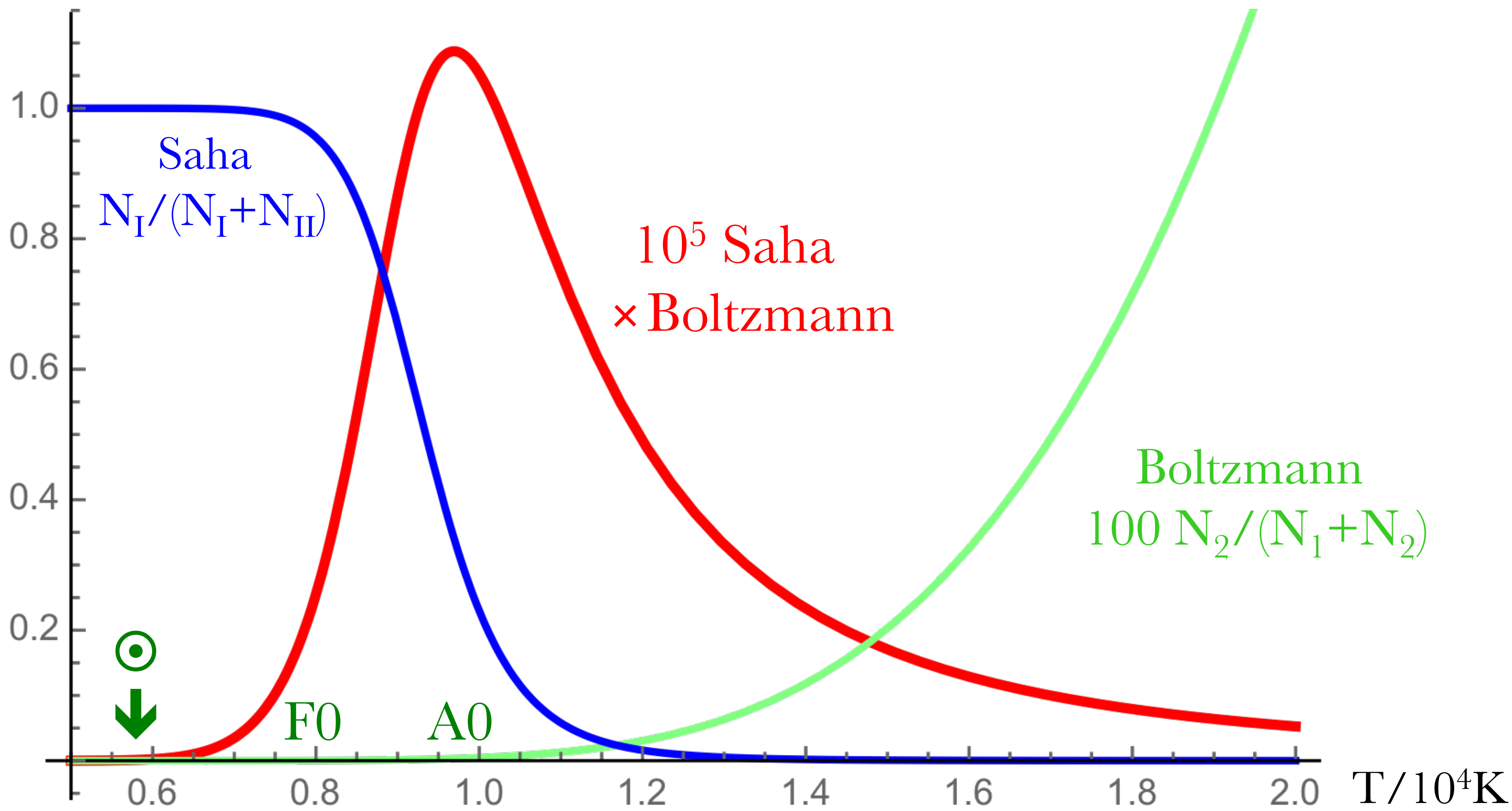

- Boltzmann excitation (green, 1-2) and Saha (neutral fraction, blue, I-II) ionization solutions for hydrogen for temperatures T in units of 10^4K. Here $n_e=10^{14}cm^{-3}$.
- Combined (red) illustrates peak Lyman L_α line signal at $T\sim10^4$K.

Hence the observed line strength is governed by the Boltzmann equation in concert with the Saha equation: for Lyman α this gives

$$\frac{N_2}{N_{\rm tot}} = \underbrace{\frac{N_2}{N_1 + N_2}}_{\text{Excitation}} \; \underbrace{\frac{N_I}{N_I + N_{II}}}_{\text{Ionization}} = \frac{N_2/N_1}{1 + N_2/N_1} \, \frac{1}{1 + N_{II}/N_I} \quad . \tag{10}$$

This peaks at $9900\,\mathrm{K}$ for hydrogen when n_e is typical of the solar surface.

Plot: Boltzmann + Saha Equation for Hydrogen

• Clearly, a delicate balance between excitation state transitions and ionization states controls line strengths, usually expressed as **equivalent widths**.

[*Reading Assignment: Example 8.1.15 from C & O, focusing on how Ca lines can dominate H lines for solar abundances*]

Plot: Spectral Line Strengths vs. T for Different Species

• The bottom line is that elemental abundances do not vary much from star to star, *yet spectral line strengths do, due to their sensitivity to* T.

• Moreover, the spectral characteristics provide powerful observational diagnostics on temperature and density, leading to cogent stellar classifications.

We can now define four different measures of a star's temperature: **C & O, p. 238**

∗ The **excitation temperature**, determined by Boltzmann's equation;

∗ the **ionization temperature**, defined by the Saha equation;

∗ the **kinetic temperature**, from the Maxwell-Boltzmann distribution,

∗ and the **color temperature**, obtained via a fit of the stellar continuum to a Planck distribution.

ATOMIC SPECTRAL LINE STRENGTHS

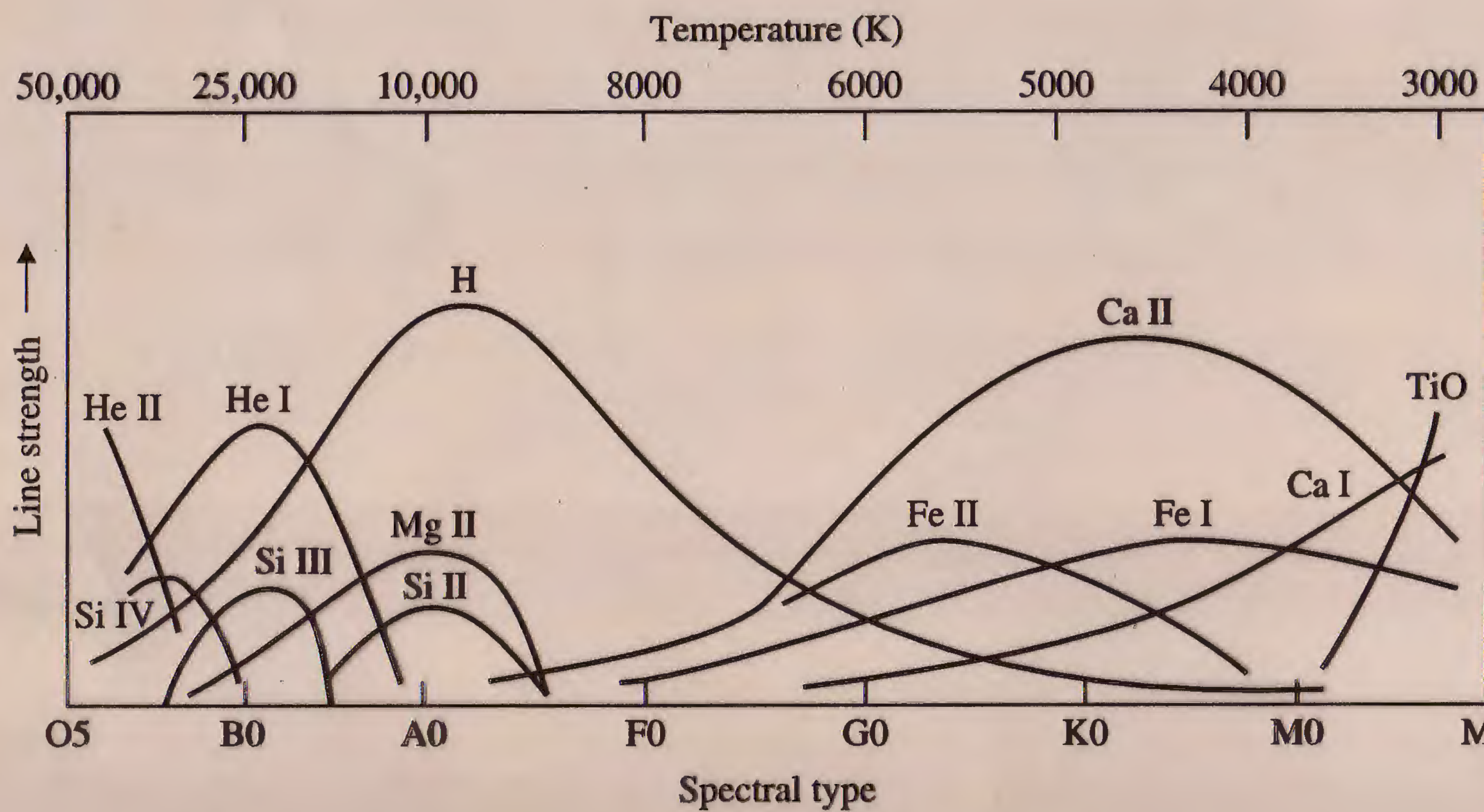

Figure 8.9 The dependence of spectral line strengths on temperature.

4 The Hertzsprung-Russell Diagram

Evidence that O stars were more massive than M stars, inferred from binary systems over a century ago, led to an incorrect evolutionary scenario: **C & O, Sec. 8.2**

$*$ that as stars age, they were thought to shed mass and exhaust their fuel before growing into old, red dim stars.

$*$ this is the early-type vs. late-type misnomer; stars do not evolve from hot, OB types to cooler GK dwarfs, as we shall discover.

• Hertzsprung in 1905, and Russell in 1913, observed a correlation between absolute magnitude M and spectral type that supported such a contention.

Plot: Russell's First Diagram

$*$ 80% – 90% of stars reside in a diagonal band called the **main sequence**.

$*$ A handful of bright, redder stars with similar spectral types but much more negative M are called (red) giants. Their larger size is inferred from the Stefan-Boltzmann law:

$$R \;=\; \frac{1}{T_{\rm eff}^2}\,\sqrt{\frac{L}{4\pi\sigma}} \quad . \tag{11}$$

• Russell's first plot was the forerunner of the modern **Hertzsprung-Russell (H-R) Diagram**, which can take either an observational (M_V vs. B-V) or theoretical (L vs. T) form.

Plot: Theorist's Hertzsprung-Russell Diagram

$*$ The radius of stars is easily inferred from the theorist's plot via diagonal "iso-radius" lines.

$*$ It is easily inferred that supergiants such as Betelgeuse ($M\sim 10M_\odot$) are very tenuous, and white dwarfs such as 40 Eridani B are very dense.

RUSSELL DIAGRAM

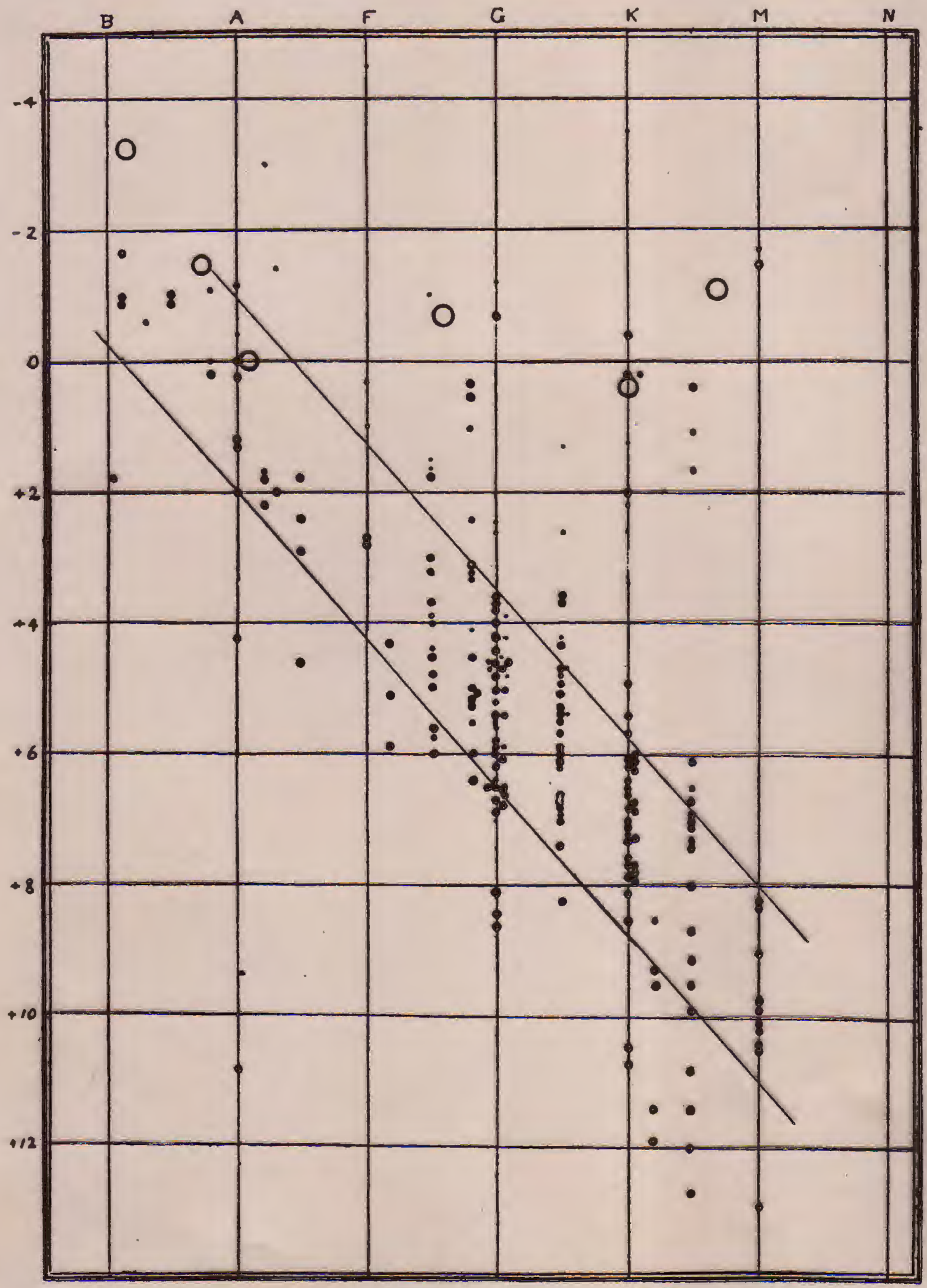

Figure 8.10 Henry Norris Russell's first diagram, with spectral types listed along the top and absolute magnitudes on the left-hand side. (Figure from Russell, *Nature*, *93*, 252, 1914.)

Stellar Hertzsprung-Russell Diagram

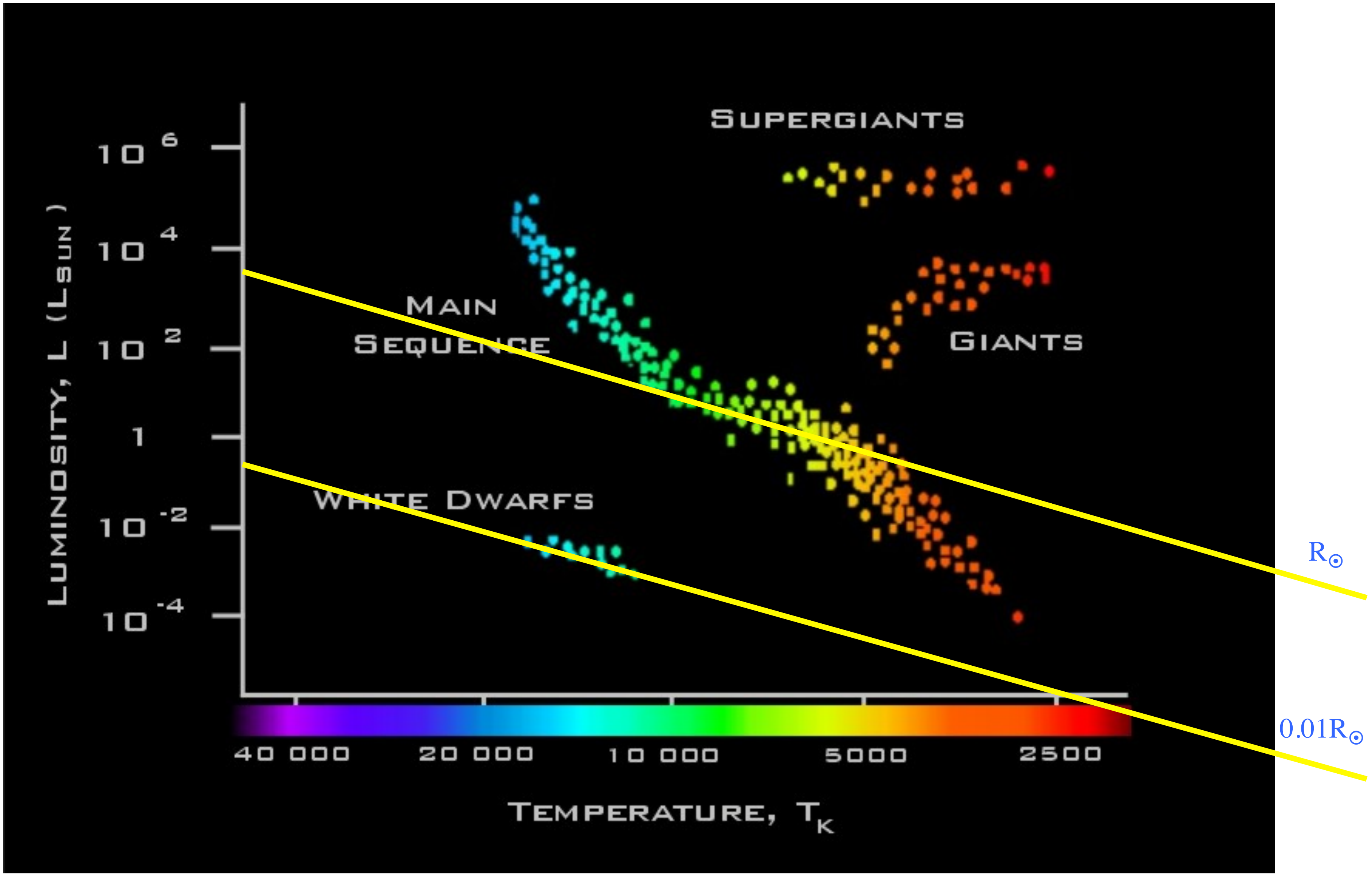

4.1 Morgan-Keenan Luminosity Classes

• Hertzsprung suggested that main sequence stars and giants of the same spectral class may possess subtle differences in their spectral lines. **C & O, pp. 246–50**

In 1943, Morgan and Keenan published their atlas of stellar spectra, identifying such subtle distinctions and defining **luminosity classes** $Ia \to VI$ for main sequence stars and giants (we now add D for dwarfs). This was the inception of the **Morgan-Keenan (M-K) classification system**.

• The comparison of strengths of two closely-spaced lines (doublets) is often used to places stars in different luminosity classes.

• Now T is not the only principal parameter: line width depends also on atmospheric mass density ρ so that both feature spectroscopically.

∗ The sun is a G2 - V star, and Betelgeuse is an M2 - Ia star.

Plot: Luminosity Classes in the H-R Diagram

• The M-K system can use spectra to place an observed star on the H-R diagram according to its spectral similarity with other known stars. The accompanying inference of L and therefore absolute magnitude M_V can be compared with m_V to deduce an estimate of the distance d to the star. This is the method of **spectroscopic parallaxes** for distance determination. The distance uncertainty is often around a factor of 1.5, due to natural spread in the H-R diagram.

HR Diagram and White Dwarfs

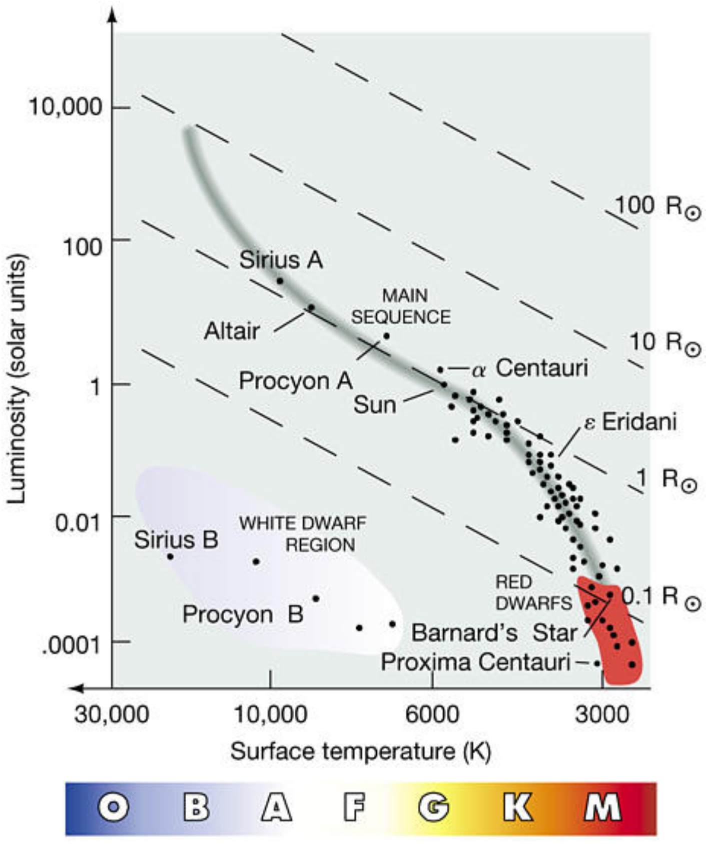

Copyright © 2005 Pearson Prentice Hall, Inc.

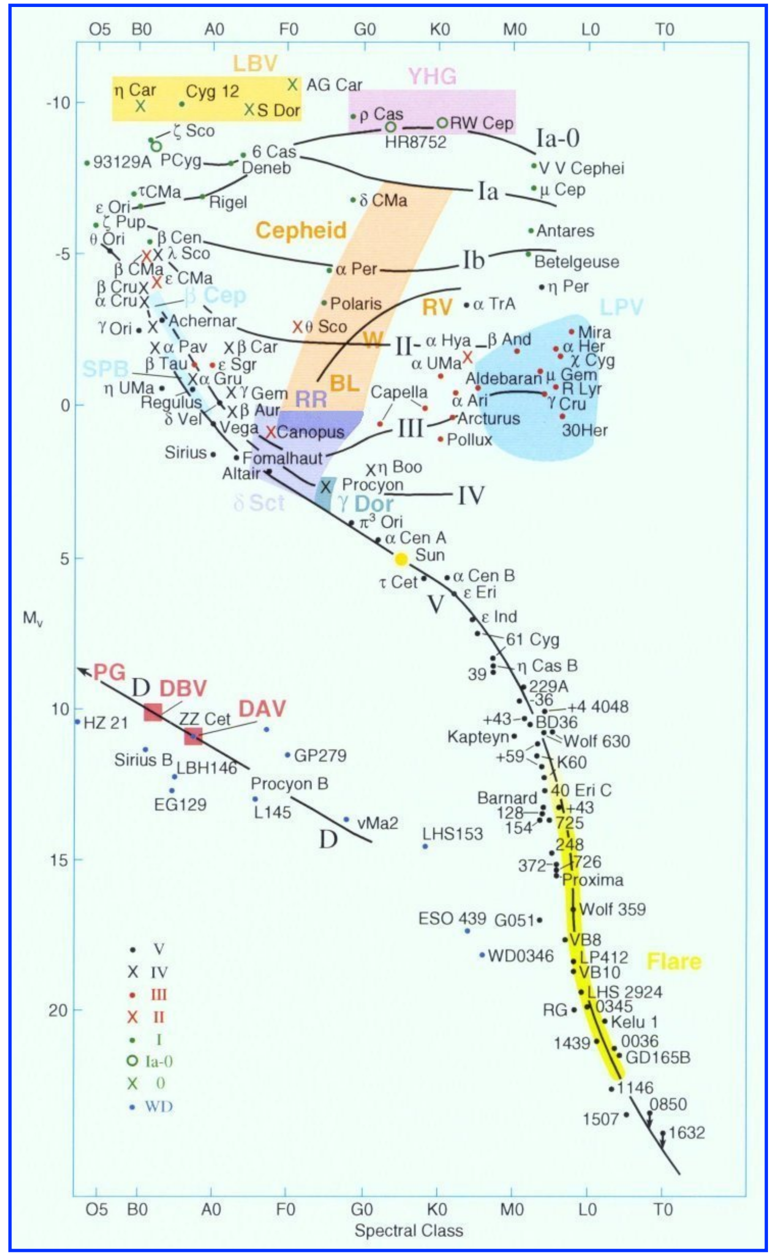

- *Left panel*: HR diagram identifying some binaries containing white dwarfs.
- *Right panel*: HR diagram with many nearby stars identified, Morgan-Keenan luminosity classes labelled, and the instability strip highlighted. [Credit: J. B. Kaler, *The Cambridge Encyclopedia of Stars*]

5 The Radiation Field

For the purposes of discussing radiative transfer, the most widely-used quantity, the **specific intensity** is defined as: **C & O, Sec. 9.1**

$$I_\lambda \; = \; \frac{dE_\lambda}{d\lambda \, dt \, dA \cos\theta \, d\Omega} \quad , \tag{11}$$

i.e., as the differential energy dE_λ per unit wavelength band $d\lambda$ crossing unit area dA at some inclination angle θ within a solid angle $d\Omega$. The geometry is as follows:

Plot: Specific Intensity Geometry

- I_λ has units of erg sec^{-1} cm^{-3} sr^{-1}.

The **mean intensity** is found by averaging over solid angles $d\Omega$, yielding

$$\langle I_\lambda \rangle \; \equiv \; \frac{1}{4\pi} \int I_\lambda \, d\Omega \; = \; \frac{1}{4\pi} \int_0^{2\pi} d\phi \int_0^{\pi} d\theta \, I_\lambda \sin\theta \quad . \tag{12}$$

In the case of blackbody radiation, since it is an isotropic radiation field, we have $\langle I_\lambda \rangle = B_\lambda$.

The rate at which photons cross the area dA is just the speed of light c, so that the energy per unit volume, or **energy density** can be simply obtained as

$$U_\lambda \; = \; \frac{1}{c} \int I_\lambda \, d\Omega \; = \; \frac{4\pi}{c} \langle I_\lambda \rangle \quad . \tag{13}$$

For blackbody radiation, we can then derive the results

$$\begin{aligned} U_\lambda \; &= \; \frac{4\pi}{c} B_\lambda \; = \; \frac{8\pi}{\lambda^5} \frac{hc}{e^{hc/\lambda kT} - 1} \\ U_\nu \; &= \; \frac{4\pi}{c} B_\nu \; = \; \frac{8\pi}{c^3} \frac{h\nu^3}{e^{h\nu/kT} - 1} \end{aligned} \tag{14}$$

and a dimensionless form can be obtained by multiplying U_ν by $h/(m_e c^2)^2$.

The Specific Intensity

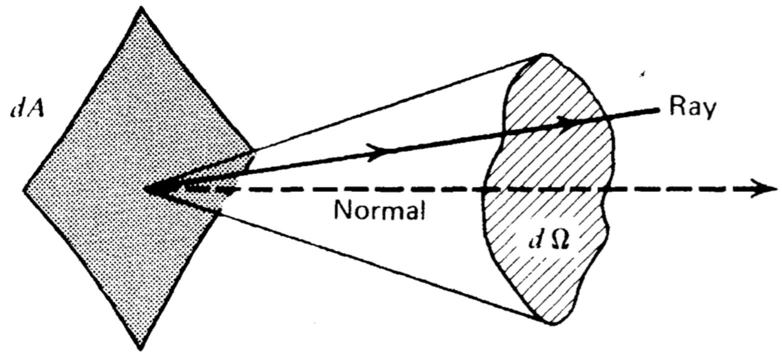

Figure 1.2 Geometry for normally incident rays.

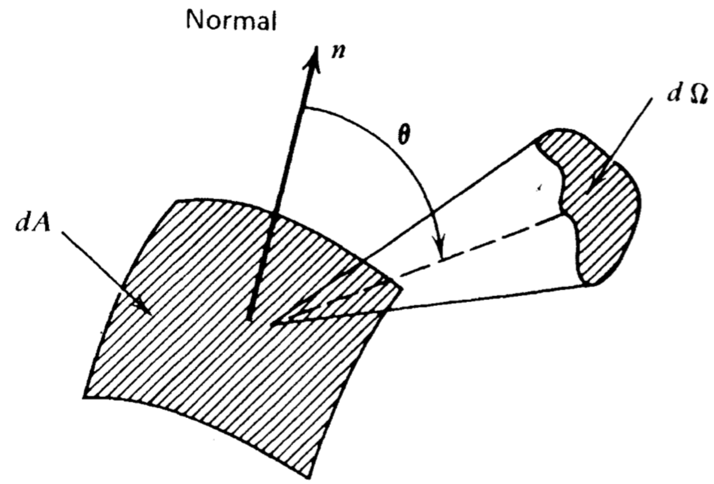

Figure 1.3 Geometry for obliquely incident rays.

The wavelength-integrated (total) energy density $U_{\rm rad}$ is then simplify obtained, and for a blackbody becomes:

$$U_{\rm rad} \;=\; \frac{4\pi}{c} \int_0^\infty B_\lambda(T)\, d\lambda \;=\; \frac{4\sigma}{c}\, T^4 \;\propto\; \frac{m_e c^2}{\lambda\!\!\!^{-}_{\rm C}^3}\, \Theta^4 \quad . \tag{16}$$

The constant $a = 4\sigma/c$ is known as the **radiation constant**. Here $\lambda\!\!\!^{-}_{\rm C} = \hbar/m_e c$ is the <u>reduced</u> Compton wavelength, and $\Theta = kT/m_e c^2$.

5.1 Radiation Pressure

Photons bouncing off a surface must exert a pressure force due to their change in momenta p. If the photons are specularly reflected at an angle θ to the normal of a surface area dA, then the change in momentum is

$$dp_\lambda \;=\; 2\,\frac{dE_\lambda}{c}\, \cos\theta \;=\; \frac{2}{c}\, \cos^2\theta\; I_\lambda\, dt\, dA\, d\Omega \quad , \tag{17}$$

which was expressed in terms of the specific intensity using Eq. (12).

The pressure is just the force per unit area, i.e. $dp_\lambda/(dt\, dA)$, so integrating over solid angles gives

$$P_{{\rm rad},\,\lambda} \;=\; \frac{2}{c} \int I_\lambda\, \cos^2\theta\, d\Omega \quad , \tag{18}$$

where it is understood that the solid angle integration is over a hemisphere.

• For isotropic radiation fields, this is trivially integrated to yield $(4\pi/3c)\, I_\lambda$. Integrating over the Planck distribution yields

$$P_{\rm rad} \;=\; \frac{4\pi}{3c} \int_0^\infty B_\lambda(T)\, d\lambda \;=\; \frac{4\sigma}{3c}\, T^4 \;\equiv\; \frac{U_{\rm rad}}{3} \quad , \tag{19}$$

where the total radiation energy density $U_{\rm rad}$ is obtained by integrating Eq. (15) over wavelengths, i.e. see Eq. (16). So the blackbody radiation pressure is one third of its energy density (c.f. for the ideal monatomic gas, this ratio is 2/3); this reflects the relativistic equation of state.